Time Domain Modal Identification/Estimation of the Mini-Mast Testbed

Michael J. Roemer† *and* **D. Joseph Mook***

Department of Mechanical and Aerospace Engineering
State University of New York at Buffalo
Buffalo, New York 14260

Abstract

The Mini-Mast is a 20 meter long, 3-dimensional, deployable/retractable truss structure designed to imitate future trusses in space. This structure has undergone various static and dynamic experiments at NASA Langley Research Center to identify its modal properties so that control laws can be developed and tested. This paper presents results from a robust (with respect to measurement noise sensitivity), time domain, modal identification technique for identifying the modal properties of the Mini-Mast structure even in the face of noisy measurements. Three testing/analysis procedures are considered: (1) sinusoidal excitation near the resonant frequencies of the Mini-Mast, (2) frequency response function averaging of several modal tests, and (3) random input excitation with a free response period. The results indicate that the robust technique of the paper is more accurate using the actual experimental data than existing techniques.

Introduction

Recently, many experimental modal analysis (EMA) techniques have been developed to improve current modal testing and analysis procedures. Modal analysis techniques can usually be classified as either frequency or time domain procedures. Some experimental difficulties arise in the frequency domain when the natural frequencies of a system are closely distributed and/or the system contains a high

† Graduate Research Assistant
* Assistant Professor

degree of damping. In the time domain, noisy output measurements are the most troublesome for accurate modal identification. However, both time and frequency domain methods encounter the most difficulty when particular modes are poorly excited during a testing procedure. For this case, the amplitudes of the poorly excited modes can be less than the RMS amplitude of the noise. In this paper, a time-domain identification algorithm which is robust with respect to measurement noise is used to identify some of the primary modes of the Mini-Mast Testbed at NASA's Langley Research Center.

The modal identification algorithm used in this paper combines the ERA identification/realization technique [1] with an optimal state estimation algorithm called MME [2] to successfully identify modal properties of a structure even in the face of noisy measurements. The ERA technique is based on the singular value decomposition of a generalized Hankel matrix composed of discrete, time-domain measurements. This time-domain technique is capable of accurately identifying modal parameters for cases involving perfect or low-noise measurements. However, difficulties may arise when high noise levels are present in the output measurements. Thus, by combining the MME optimal state estimation algorithm with the ERA identification algorithm, improved modal identification is achieved through lowering the algorithm's sensitivity to noise. This ability has been demonstrated in numerous simulations of different test systems [3-6].

The Minimum Model Error (MME) estimation algorithm is well suited for the modal identification problem because it does not assume that the model error is a white noise of known covariance as do other estimation filters (e.g., Kalman filter). Instead, the model error is assumed to be an unknown quantity and is estimated as part of the solution. The theoretical advantages of this assumption are obvious for the present problem, since the model is unknown *apriori*. Since the model is comprised of deterministic modes, the identification problem is one of finding (eliminating) deterministic model error. In several previous studies, the MME has been shown to produce state estimates of high accuracy for problems involving both significant model error and significant measurement error [7].

Reducing the noise sensitivity of the Eigensystem Realization Algorithm has been investigated in several computer simulations. The results were based on 3 and 4 mode simulated truths to which gaussian distributed white noise was added to simulate noisy measurements. The ERA was found to be extremely accurate at low noise levels. However, the accuracy is diminished if the measurement noise is increased enough to effect the lower amplitude modes. This result was also reported by Juang and Pappa [8]. However, compared with ERA by itself, the

combined ERA/MME algorithm produced more accurate results with respect to identifying the number of modes, frequencies, damping ratios, and mode shapes. For example, in a 4 mode simulation example using noisy measurements with a variance of 0.004, the ERA algorithm could only identify 3 of the 4 modes. The combined ERA/MME algorithm, on the other hand, identified all 4 modes and their respective mode shapes accurately [4]. The purpose of this paper is to extend this theoretical/simulation background to the Mini-Mast CSI testbed, in order to examine its identification ability on actual experimental data taken from a large space structure.

Mini-Mast Testing Procedure

The Mini-Mast is a deployable/retractable test truss structure designed to imitate future trusses to be used in space. A representative illustration supplied by NASA is shown in Figure 1. The Mini-Mast is approximately 20 meters in length (18 bays, 1.12 meters each), and has a three-longeron construction forming a triangular cross-section with points inscribed by a circle of 1.4 meters in diameter [10]. The truss is cantilevered vertically to the ground by bolting the lowest three joints. The joints are made of machined titanium (6A1-4V) to hinge the longeron and diagonal members securely. The tubing members are constructed of a graphite/epoxy composite. The Mini-Mast has undergone various static and dynamic experiments. The work of this paper is concentrated on the data taken from selected dynamic tests.

Several types of response sensors are available on the Mini-Mast testbed. The sensors chosen for the dynamic tests discussed here are Kaman KD-2300 displacement probes. The probes are positioned to measure deflections orthogonal to the face of the probe, and are mounted in parallel to the Mini-Mast's corner joints. All of the bays except bay 1 are instrumented with three of these displacement sensors. The operating principle of the sensors is based on the impedance variations caused by eddy currents induced in a conductive metal target. The displacement is sensed from the coupling between a coil in the sensor and a particular target. Resolution of the Kaman KD-2300-10CU at mid range is 0.0025 mm, with a static frequency response up to 50 kHz

Three testing/analysis procedures are examined. First, frequency response functions (FRF) were constructed from (1) a finite element model, and (2) experimental data supplied by NASA's Spacecraft Dynamics Branch. A plot illustrating the type of data used in this analysis is shown in Figure 2.

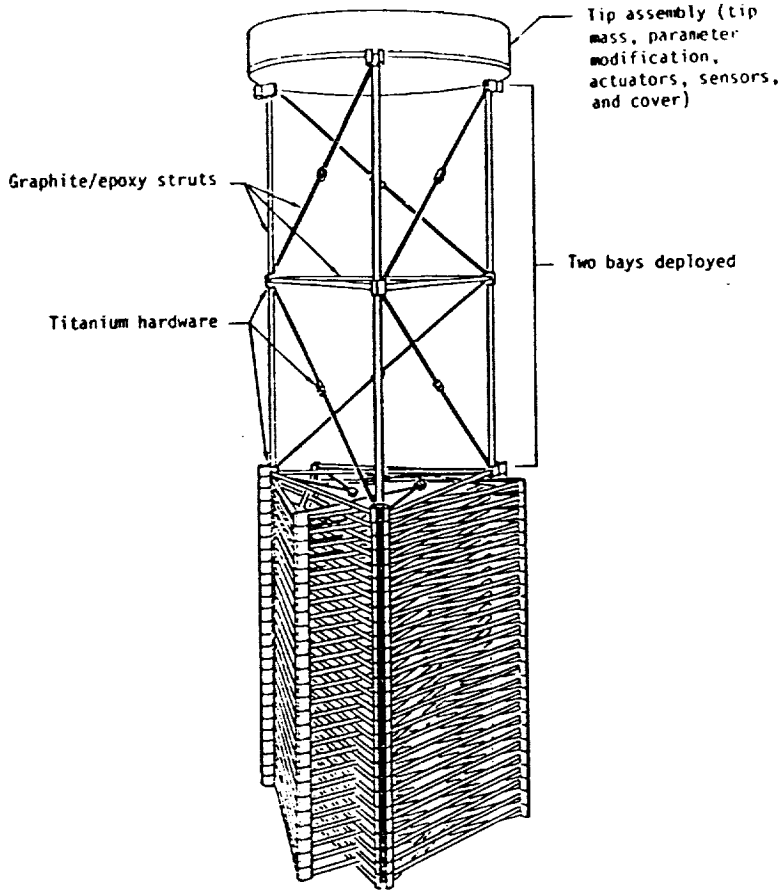

Figure 1 NASA's Mini-Mast Testbed

Referring to Figure 2, the frequency response function distinguished by the crosses represents the finite element or analytical model. The remaining frequency response function is derived from many sets of experimental data and generated using SDRC's I-DEAS test analysis package. The first analysis procedure discussed in this paper identifies the modal properties of the Mini-Mast structure by taking inverse fourier transforms of the averaged FRF's and using them as input to the identification algorithm. The identified natural frequencies establish a "truth" for comparing the other identification and testing procedures. The second testing procedure consisted of exciting the Mini-Mast test structure at frequencies close to its predicted natural frequencies. The time domain responses are then transformed into the frequency domain where a transfer function is formulated using auto and cross correlations. Finally, the impulse response (to be analyzed) is found by transforming back to the time domain. The third testing/analysis procedure consisted of randomly exciting the Mini-Mast structure and then allowing it to free decay until it comes to rest. Three response points were monitored at bay 10 at a sampling

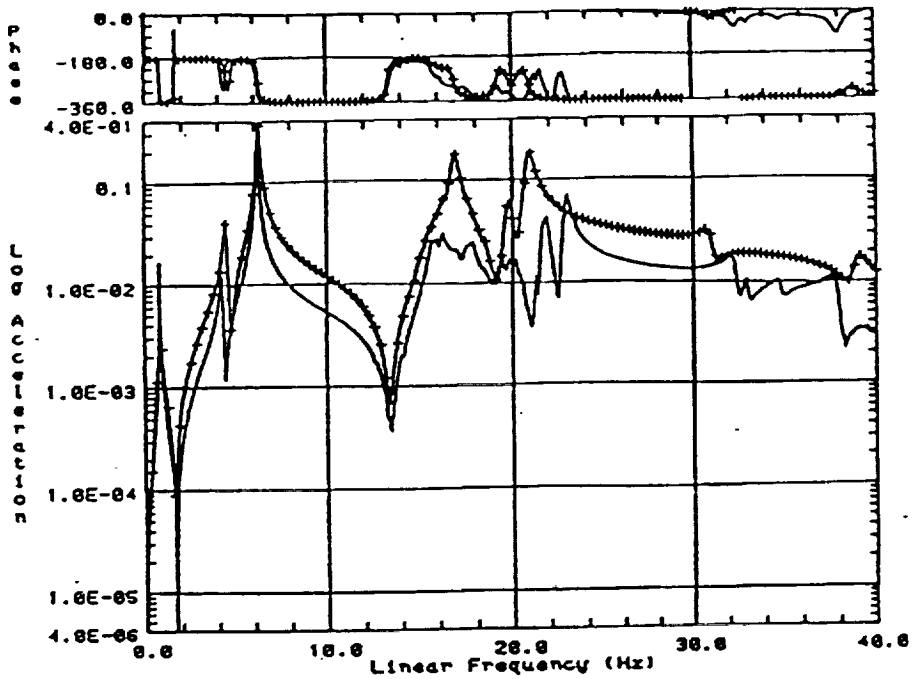

Figure 2 Example Frequency Response Function

rate of 128 Hz The response portion used in the identification/estimation algorithm included 100 data points from the free response of the structure. The combined ERA/MME algorithm was compared against the ERA by itself. The results were compared with respect to the following criteria: (1) the "truth" established by the frequency response function averaging, (2) damping ratio identification, and (3) modal amplitude coherence factors. Improvements were noted with respect to all three performance measures.

Frequency Response Function Analysis

The inverse fourier transforms of select frequency response functions were obtained to get a representative impulse time history. This impulse response data was then filtered so that a small frequency bandwidth could be investigated closely. The first frequency bandwidth considered was 0 Hz to 10 Hz. In this region, the first and second bending modes were observed as well as the first torsion mode. Included in the frequency range of 10Hz to 20 Hz are a cluster of 108 "local" modes. These modes are primarily due to the bending of the 54 diagonal truss members. The final frequency range considered was 20 Hz to 30 Hz. In this range, the second torsion mode was identified. The transformed time-domain data was used as input to the combined ERA/MME algorithm. A summary of the steps associated with

this experimental analysis is provided below.

Modal Identification Algorithm

1. Obtain time-domain measurements from either the inverse transforms of the frequency response functions or raw data from the Mini-Mast.

2. Apply the Eigensystem Realization Algorithm (ERA) to the measurements obtained from the Mini-Mast test structure.

3. Input a realized model and the measurements into the Minimum Model Error (MME) algorithm to produce optimal state estimates.

4. Sample the MME produced state estimates at discrete-time intervals to create simulated measurements of higher accuracy than the original measurements.

5. Apply ERA to the simulated measurements in order to realize/identify the new modal parameters.

6. Examine the identified modal parameters for some convergence criteria, and repeat the procedure if necessary.

The first two bending and torsion modes of the Mini-Mast were isolated as modes of particular interest in this paper. Utilizing a 10^{th}-order, Butterworth, low-pass filter, the first two bending modes and the first torsion mode were clearly identified using the FRF data. Because the exact frequencies of the Mini-Mast are unknown, a small range is given for each identified frequency to serve as the "truth". Using the fourier inverse of several averaged data sets, the first bending mode was identified in the range of 0.87 - 0.88 Hz, the first torsion mode between 4.20 - 4.35 Hz, and the second bending mode was in the range of 6.25 - 6.35 Hz The second torsion mode was identified with the help of a 10^{th}-order, Butterworth, band-stop filter. A band-stop filter was chosen in order to filter out the effects of the 108 "local" modes in the frequency range of 10 to 20 Hz The identified natural frequency of this mode was between 22.1 - 22.7 Hz. An illustration of the frequency and time domain equivalents used in this analysis are shown in Figures 3 and 4.

The identification results presented above are produced from the combined ERA/MME algorithm. However, the ERA algorithm alone produced the same results. This result is expected because the frequency response functions were formed from an average of several tests. Also, the averaged FRF's were filtered to iso-

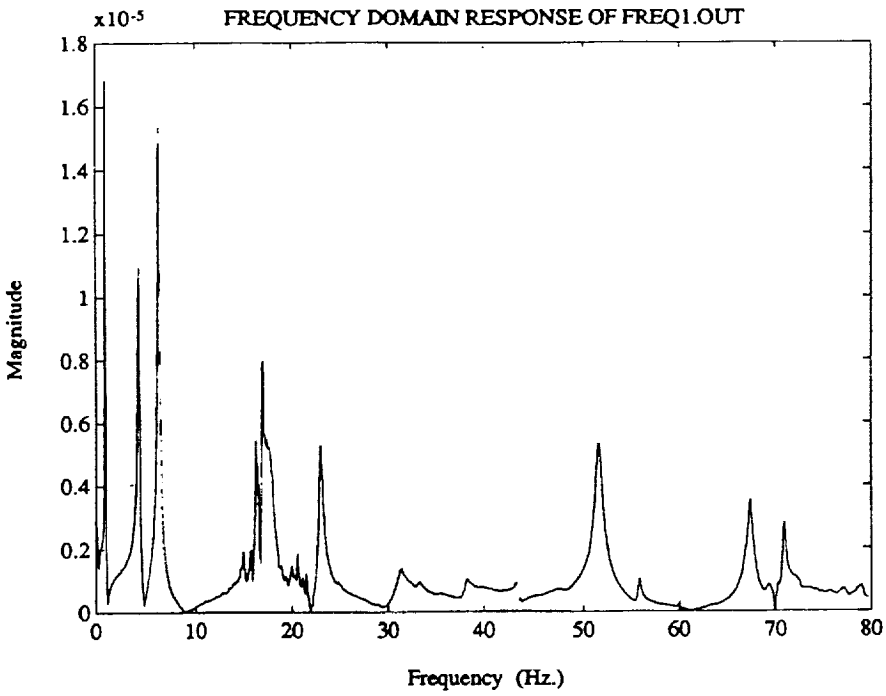

Figure 3 Frequency Response

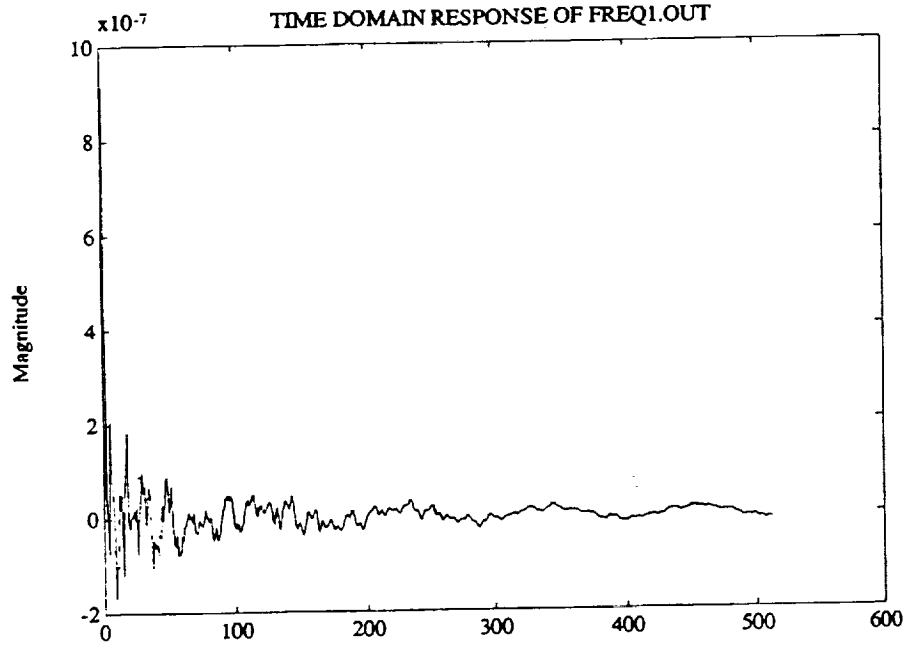

Figure 4 Impulse Response

late the particular modes to be identified. The ranges of the Mini-Mast's first four

natural frequencies of interest are given below.

$$\omega_{b1} \approx 0.87 - 0.88 \quad Hz$$
$$\omega_{t1} \approx 4.20 - 4.35 \quad Hz$$
$$\omega_{b2} \approx 6.25 - 6.35 \quad Hz$$
$$\omega_{t2} \approx 22.1 - 22.7 \quad Hz$$

Sinusoidal Excitation Analysis

In this section, sinusoidal excitations are applied to the Mini-Mast test structure. The frequencies of the sinusoidal forces are set near the assumed natural frequencies of the structure in an attempt to produce a more accurate identification. A torque wheel located at the top of the mast was used to excite the structure, while the Kaman displacement probes sensed the structure's motion. Once the measurements from the input and output sensors are collected, a transfer function of the Mini-Mast can be constructed. The transfer function equation is composed of cross and auto correlations as:

$$G(j\omega) = \frac{S_{xx}(\omega)}{S_{fx}(\omega)}$$

where

$$S_{xx} = auto - spectral\ density$$
$$S_{fx} = cross - spectral\ density$$
$$G(j\omega) = frequency\ response\ or\ transfer\ function$$

This equation is based on the fast fourier transform of the input/output time histories. Excluding the initial transient response of the structure due to the torque wheel force, the frequency response is dominated by the frequency of excitation. Because of this, a mathematical problem exists when computing the system's transfer function. More specifically, at frequencies other than the excitation frequency, the fourier transform of the input produces numbers very close to zero. Therefore, a problem of dividing by numbers that are very close to zero is unavoidable. To overcome this difficulty, a small amount of gaussian distributed white noise with variance of $4x10^{-6}$ was added to the measurements. As expected, the addition of white noise produced larger numbers in the frequency response of the structure at frequencies other than the excitation frequency. After the transfer function is

formulated, the impulse response can be generated for input to the identification algorithm. The impulse response is calculated by taking the inverse fourier transform of the structure's transfer function or FRF.

The modal identification procedure started by using the ERA by itself. Individual input/output time histories were used to construct a 100x100 Hankel matrix, from which a 12^{th}-order model was realized. An average of 5 tests were used to arrive at the identified frequencies for both the ERA and ERA/MME algorithms. Most of the individual time histories only revealed information about a couple of the modes at one time. Therefore, several different time histories were used to formulate each identified natural frequency.

The ERA/MME identification algorithm takes advantage of the realized model ERA produces in order to robustly identify a structure's modal properties. More specifically, the realized model is used in the MME estimation scheme to smooth the measurements. However, a concern of particular importance is how much error is present in the realized model. The realized model was produced from undoubted noisy measurements and truncated modes. The fact that model error is often composed of truncated modes makes the common estimation assumption of using white noise for model error particularly poor. Minimum Model Error (MME) estimation addresses this concern by estimating the model error as part of the solution. The model error is assumed as part of the solution, so no assumptions (such as white noise) are required. Instead of the need to assume both measurement and model error covariances, as in the case of the Kalman filter, only the measurement error covariance is needed. In addition, a study performed in reference [11] concluded the following important result. When predicting the measurement error covariances (the *only* input covariance needed for the ERA/MME algorithm), it is important to predict a low covariance in the beginning and slowly increase the prediction until the best modal amplitude coherence factors are found. The reason for this is that if the predicted measurement error covariance is lower than the unknown actual measurement error covariance, then the estimate can never be worse than the measurements are already. This result allows the user to have faith when implementing the ERA/MME algorithm. However, if the predicted measurement error covariance is higher than the unknown actual measurement error covariance, then the simulated measurements from the estimates could become worse (more noisy) than the original measurements. Because of this, it is important to assume measurement error covariances low when satisfying the covariance constraint of the MME estimation technique

Following the six step procedure of the ERA/MME algorithm, only two

iterations were used for identifying the first four natural frequencies. Simple one- and two-mode models were used in the estimation/identification scheme. The use of these truncated models highlights the importance of not modeling the truncated modes as white noise. A table illustrating all of the results is given below.

Table 1 Sinusoidal Analysis Result Comparison

	"Truth"	ERA	ERA/MME
	frequency (Hz)	frequency (Hz)	frequency (Hz)
1 bending	0.87 - 0.88	0.8470	0.8668
1 torsion	4.20 - 4.35	4.1175	4.4027
2 bending	6.25 - 6.35	7.0457	6.8943
2 torsion	22.1 - 22.7	22.150	22.091

Comparing the ERA and combined ERA/MME algorithms with the FRF analysis results indicates an overall improvement when using the combined procedure. More specifically, identification accuracy of the first three frequencies identified by the ERA/MME algorithm were improved by up to 5% over ERA by itself. The fourth frequency remained basically the same.

Using available NASA data, inverse and regular fourier transformations were performed in order to get the impulse time histories needed for time domain modal identification. Transformed and filtered data is not the type of data the ERA/MME identification/estimation procedure was intended for use on. This is because the noise that might have been present in the original test data would have been altered significantly by these transformations etc. Therefore, the improved results (using MME estimation) were not as significant as might be expected if raw impulse response data or data generated from random input excitations were available. Using raw data is the next step for testing the ERA/MME algorithm.

Random Excitation/Free Response Analysis

In this section, the Mini-Mast test structure was excited using a random

input with a bandwidth ranging from 0 to 40 Hz. The random excitation was applied for 26 seconds and then the structure was allowed to free respond until the response went to zero. Three response points were monitored at bay 10 of vortices A, B, and C, and the shaker was located at bay 9. The data sampling rate was 128 Hz and the free response portion of the time history began at the 33 second mark. The response portion that was used in the identification/estimation algorithm included 100 data points ranging in time from 34.0 to 34.8 seconds. The combined ERA/MME identification algorithm was compared against ERA by itself to examine the advantages of the combined technique. A predicted noise variance of 1×10^{-12} was used in the MME estimation scheme to satisfy the covariance constraint.

To examine if the results of the combined ERA/MME algorithm are better than the ERA identification results, the modal amplitude coherence (MAC) factors were calculated for each mode. MAC's estimate the degree of modal excitation or controllability for each mode. A MAC factor close to 1 means that the mode was identified well during the testing procedure. As shown in Tables 2 through 5, the MAC factors are indeed improved for all four primary modes. The damping ratios also seem to be improved, assuming that the damping ratios of the Mini-Mast are less than 5% (a reasonable assumption for such a structure). For example, the damping ratio of the first torsional mode identified by ERA was 0.101 and the ERA/MME identified it to be 0.0044. Note, the most improved damping ratios and MAC factors were found to be associated with the torsional modes of the Mini-Mast. This can be explained by the fact that the shaker was used in only one direction. Therefore, the linear or bending modes were excited more rigorously than the torsional modes. This result highlights a major advantage of using the combined ERA/MME algorithm, namely to help identify modes not excited very well in a testing procedure.

First, let's examine the identification results of the responses at bay 10, vortex A as shown in Tables 2 and 3. Improvements were made with respect to the MAC factors for all four primary modes. However, a more distinct improvement was observed when identifying the 2 torsional modes. Specifically, the first torsional mode's MAC factor as identified by ERA was 0.8974, while the ERA/MME identified MAC factor was increased to 0.9842. The MAC factor of the second torsional mode was identified by ERA as 0.8633, and the ERA/MME algorithm improved it to 0.9457. The improved MAC's are also supported by the identified frequencies and damping ratios. The "true" torsional frequencies were identified by the averaged FRF's in the range of 4.20 - 4.35 Hz and 22.1 - 22.7 Hz. The torsional modes identified by ERA were 4.77 Hz and 22.61 Hz respectively, and those identified by

the combined algorithm were 4.37 Hz and 22.4 Hz respectively, a supportive conclusion. The damping ratio of the first torsional mode identified by ERA was over 10% and the ERA/MME technique reduced it to 0.4%. Hence, when examining the MAC factors, natural frequencies, and damping ratios, the combined algorithm produced improvements with respect to each one.

The identification results from the responses at bay 10, vortex B are given in Tables 4 and 5. The MAC factors for each identified mode are again improved, but not as significant as in the previous case. The most improved mode was the first torsional mode. The MAC factor identified by ERA was 0.9546, while the ERA/MME algorithm improved it to 0.9719. The natural frequency associated with this mode was identified by ERA to be 4.56 Hz and the ERA/MME procedure identified it to be 4.39 Hz. Recall, the "true" natural frequency identified by the averaged FRF's was in the range of 4.20 - 4.35 Hz. The damping ratio was also reduced from 2.87% (using ERA) to 0.72% (using ERA/MME).

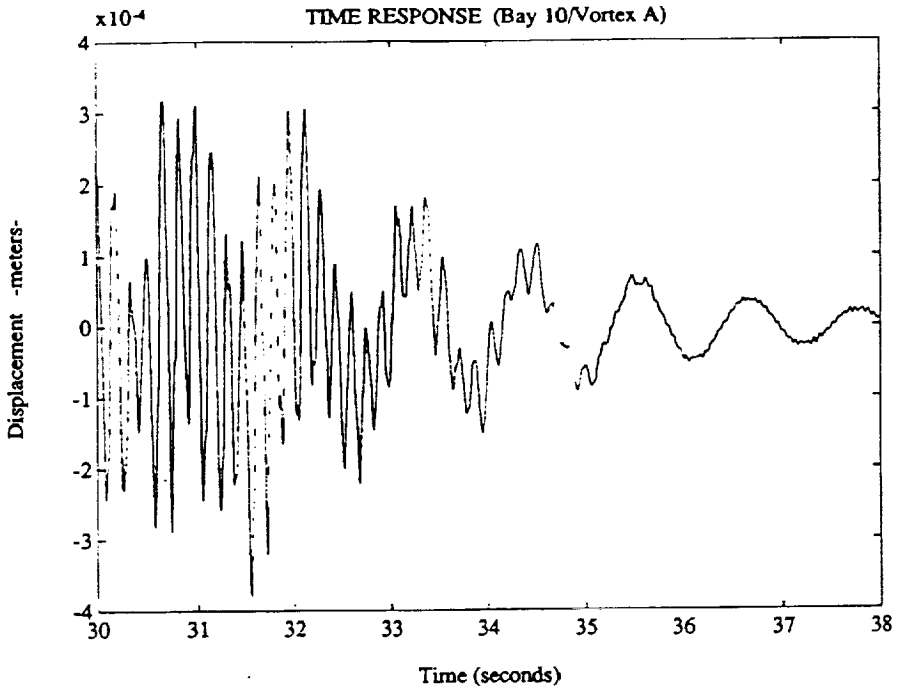

Figure 5 Output Vortex A

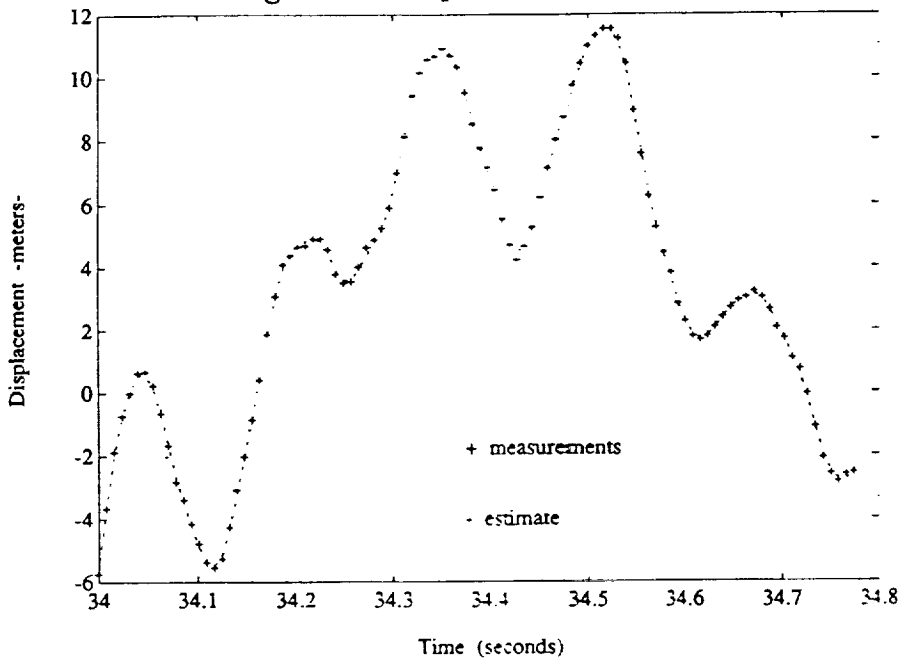

Figure 6 Estimate and Measurements Vortex A

Table 2 ERA Vortex A Results

	"Truth"	ERA		
	frequency (Hz)	frequency (Hz)	damping ratio	MACF (0-1)
1 bending	0.87 - 0.88	0.8821	0.0377	0.9981
1 torsion	4.20 - 4.35	4.7713	0.1019	0.8974
2 bending	6.25 - 6.35	6.1479	0.0287	0.9901
2 torsion	22.1 - 22.7	22.607	0.0322	0.8633

Table 3 ERA/MME Vortex A Results

	"Truth"	ERA/MME		
	frequency (Hz)	frequency (Hz)	damping ratio	MACF (0-1)
1 bending	0.87 - 0.88	0.8814	0.0240	0.9993
1 torsion	4.20 - 4.35	4.3719	0.0044	0.9842
2 bending	6.25 - 6.35	6.2156	0.0299	0.9962
2 torsion	22.1 - 22.7	22.443	0.0164	0.9457

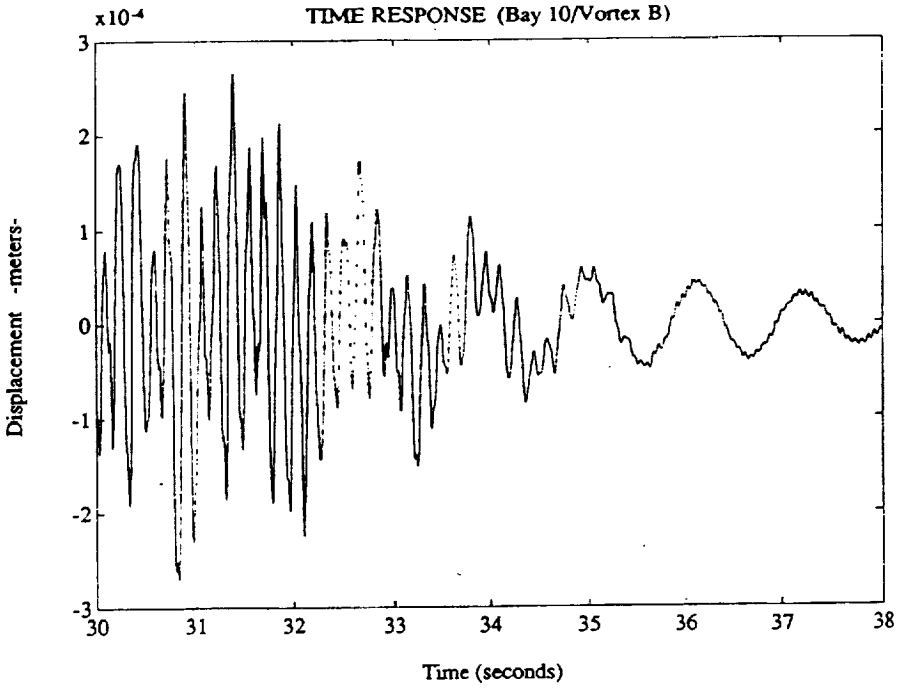

Figure 7 Output Vortex B

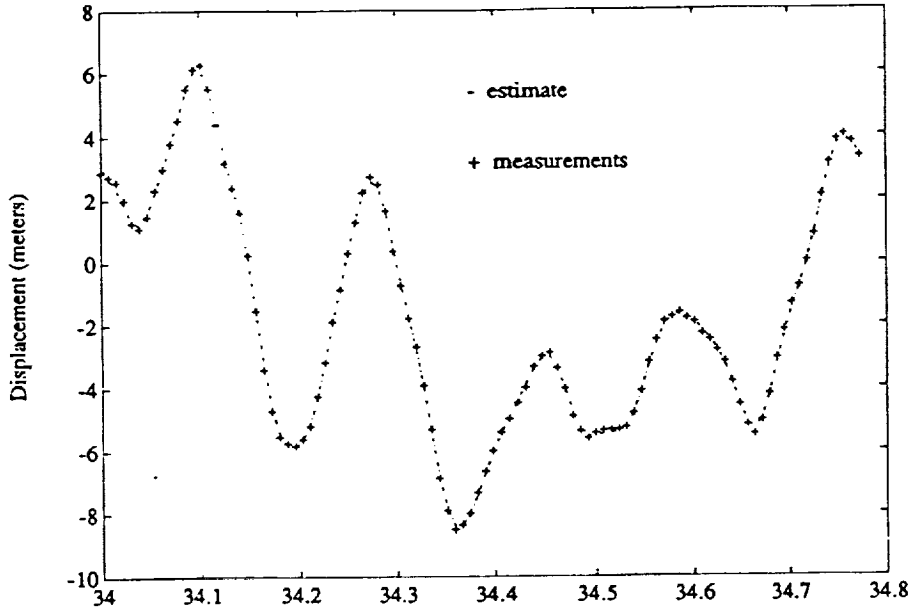

Figure 8 Estimate and Measurements Vortex B

Table 4 ERA Vortex B Results

	"Truth"	ERA (b)		
	frequency (Hz)	frequency (Hz)	damping ratio	MACF (0-1)
1 bending	0.87 - 0.88	0.8585	0.1206	0.9914
1 torsion	4.20 - 4.35	4.5576	0.0287	0.9546
2 bending	6.25 - 6.35	6.2174	0.0209	0.9925
2 torsion	22.1 - 22.7	22.324	0.0283	0.9472

Table 5 ERA/MME Vortex B Results

	"Truth"	ERA/MME (b)		
	frequency (Hz)	frequency (Hz)	damping ratio	MACF (0-1)
1 bending	0.87 - 0.88	0.8590	0.1217	0.9930
1 torsion	4.20 - 4.35	4.3978	0.0072	0.9719
2 bending	6.25 - 6.35	6.2004	0.0211	0.9955
2 torsion	22.1 - 22.7	22.227	0.0272	0.9488

Mini-Mast Identification Summary

Three different modal testing techniques for identifying some of the primary modes of NASA's Mini-Mast testbed were examined. The frequency response function analysis served to create a "truth" which the sinusoidal excitation and impulse response tests could be compared against. The authors believe the "truth" is accurate because of the many tests that produced the averaged results. The sinusoidal testing procedure included adding white noise to the original measurements so that a transfer function could be approximated. The transfer functions were then transformed into the time domain for input to the identification algorithms. Results from the identification algorithms revealed improvements (up to 5%) in identifying the first three natural frequencies of the Mini-Mast. The third test included shaking the Mini-Mast structure with a random input for 26 seconds and then allowing the structure to come to rest. The results of this test gave the best improvements when compared with the other tests because the developed algorithms were intended for use on raw impulse response or free response data. The other tests employed FFT's and inverse FFT's to construct the impulse responses. The identification of the torsional modes were especially improved using the combined identification/estimation algorithm. The identification improvements were based on; (1) the damped natural frequncies identified by ERA and ERA/MME being closer to the FRF averaged identified frequencies, (2) The damping ratio identification, specifically having damping ratios approximately 2% or less, and (3) the modal amplitude coherence (MAC) factors being close to 1. The most improved case was found in the identification of the first torsion mode. The ERA identified MAC factor was 0.8984 and the combined ERA/MME improved the MAC factor to 0.9842. Also, the damping of this mode was identified by ERA to be 0.1019 and the ERA/MME identified it to be 0.0044, a noticeable improvement if the damping is indeed close to 0.

The fact that the MAC factors of the torsional modes were lower than the bending modes (for both the ERA and ERA/MME identification techniques) allows us to conclude that the torsional modes were not excited very well during the modal test. This concern, along with improvements in the identification of the damping ratios and natural frequencies, was addressed by the ERA/MME identification scheme (specifically by the results of the free decay tests given in Tables 2 through 5). The combined identification/estimation algorithm can therefore improve time domain identification methods in the case of noisy output measurements or poorly excited modes.

References

1. Juang, J.-N., and Pappa, R.S., "An Eigensystem Realization Algorithm (ERA) for Modal Parameter Identification and Model Reduction", **AIAA Journal of Guidance, Control, and Dynamics**, Vol. 8, No. 5, pp. 620-627, Sept.-Oct. 1985.

2. Mook, D.J., and Junkins, J.L., "Minimum Model Error Estimation for Poorly Modeled Dynamic Systems", **AIAA Journal of Guidance, Control, and Dynamics**, Vol. 11, No. 4, pp. 367-375, May-June. 1988.

3. Mook, D.J., and Lew, J.S., "A Combined ERA/MME Algorithm for Robust System Realization/Identification", **Journal of the Astronautical Sciences** to appear.

4. Roemer, M. J., and Mook, D. J., "Enhanced Realization/Identification of Physical Modes", **A.S.C.E. Journal of Aerospace Engineering.**, Vol. 3, No. 2, pp. 122-136, April 1990.

5. Roemer, M. J., and Mook, D. J., "An Enhanced Mode Shape Identification Algorithm", 30^{th} Structures, Structural Dynamics, and Materials Conference (S.D.M.), Mobile, Alabama, April 1989.

6. Roemer, M. J., and Mook, D. J., "Robust Realization/Identification of Damped Structures", Damping 89 Conference, West Palm Beach, FL, February 1989.

7. Mook, D.J., and Lin, J.-C., "Minimum Model Error Estimation of Modal Truncation Errors", Proceedings of the 1987 Spring Meeting of the Society for Experimental Mechanics, Houston, TX, June 1987.

8. Juang, J.-N., and Pappa, R.S., "Effects of Noise on Modal Parameters Identified by the Eigensystem Realization Algorithm", **AIAA Journal of Guidance, Control, and Dynamics**, Vol. 9, No. 3, pp. 294-303, May-June, 1986.

9. Lew, J.S., and Mook, D.J., "Two-Point Boundary Problems Containing Jump Discontinuities", in Review.

10. Pappa, R., Miserentino, B., Bailey, J., Elliot, K., Perez, S., Cooper, P., Williams, B., Suul, J., Ghosh, D., Montegomery, R., "**Mini-Mast CSI Testbed Users Guide**", NASA Langley Research Center, Hampton, VA.

11. Roemer, M. J., "Robust System Realization/Identification via Optimal State Estimation", Ph.D. Dissertation, S.U.N.Y at Buffalo, 1990.

12. Vold, H., Kundrat, J., Rocklin, G. T., and Russell, R., "A Multiple Input Modal Estimation Algorithm for Minicomputers", SAE paper number 820194, 1981.

13. Inman, D. J., **Vibration with Control, Measurement, and Stability**, Prentice-Hall Inc., New Jersey, 1989.

14. Kalman, R.E., "A New Approach to Linear Filter and Prediction Problem", **Trans. ASME, J. Basic Engr.**, Vol. 82, pp 34-45, 1960.

	"Truth"	Low-Pass Filtered ERA @Vortex A (f = 40 Hz)		
	frequency (Hz)	frequency (Hz)	damping ratio	MACF (0-1)
1 bending	0.87 - 0.88	0.8731	0.0622	0.9942
1 torsion	4.20 - 4.35	4.3591	0.0311	0.9266
2 bending	6.25 - 6.35	6.3199	0.0268	0.9855
2 torsion	22.1 - 22.7	22.343	0.0443	0.7489

	"Truth"	Low-Pass Filtered ERA @Vortex B (f = 40 Hz)		
	frequency (Hz)	frequency (Hz)	damping ratio	MACF (0-1)
1 bending	0.87 - 0.88	0.8396	0.0211	0.9489
1 torsion	4.20 - 4.35	4.5066	0.2984	0.8797
2 bending	6.25 - 6.35	6.2918	0.0573	0.9853
2 torsion	22.1 - 22.7	21.240	0.0825	0.7792